

# Design of TPMS-based Uniform and Hybrid Graded Lattice Structures: A Fluid Flow Analysis

Rajkumar<sup>1</sup>, Janakarajan Ramkumar<sup>1\*</sup>, and Kantesh Balani<sup>2</sup>

<sup>1</sup>Department of Mechanical Engineering, Indian Institute of Technology Kanpur, Kanpur-208016, India

<sup>2</sup>Department of Materials Science and Engineering, Indian Institute of Technology Kanpur, Kanpur-208016, India

**Abstract.** Each year, more than four million people around the world undergo bone grafts and prosthesis transplants to treat bone defects and injuries by repairing and/or replacing native bone. As a result, the scaffold holds great promise for the regeneration of damaged or diseased bone tissues. One of the key components is the design of scaffolds that can mimic the structure and function of natural bone. Based on unit cell design, triply periodic minimal surface (TPMS) has attracted the attention of researchers for designing porous scaffolds. In current study, uniform and multi-morphology hybrid graded structures were designed based on TPMS, namely, primitive and I-graph-wrapped package (IWP) minimal surfaces. Furthermore, a computational fluid dynamic (CFD) model was designed based on COMSOL Multiphysics to understand the fluidic characteristics (permeability and wall shear stress) of the structures. The results show that structures reported a permeability of  $7.4 - 14.3 \times 10^{-8} \text{ m}^2$ , meeting the requirements of natural bone. Moreover, the average wall shear stress of  $0.5 - 136 \text{ mPa}$  was observed, suitable for osteoblast differentiation and proliferation.

## 1 Introduction

Bone is a type of connective tissue that has a self-healing capacity. It has complex internal and external structures (different shapes and sizes) and forms the structural framework of the vertebrate skeleton [1]. When the bone defect size increases, the self-healing capacity of the bone becomes limited [2]. Treating bone defects with traditional surgical operation methods are difficult. It is because of morbidity at the donor site, autografting scarcity, and allografting that create the risk of infection and diseases [2,3]. To overcome these consequences, bio-scaffold i.e., bone tissue engineered scaffold can act as the novel strategies to restore biomechanical stability and promote bone regeneration. A scaffold of complex porous structure can help in cell adhesion and proliferation to mimic native bone. The scaffolds can be designed based on a unit-cell design that is repeated throughout the scaffold. The unit cell designs are characterized by parametric mathematical equations that define the geometry of the unit cell and control the porosity with specific pore shape and size [4]. In recent years, based on unit cell design, triply periodic minimal surfaces (TPMS) have gained significant attention in the field of bone tissue engineering. TPMS lattices are mathematical models of

\*Corresponding author: [jrkumar@iitk.ac.in](mailto:jrkumar@iitk.ac.in)

complex three-dimensional structures which are repeated periodically in three dimensions and have minimal surface area within the boundaries [5]. To date, many TPMS minimal surface were utilized in designing of porous scaffold as an implant to treat the bone defects. When the unit cell/relative density varied spatially within the structure, it is referred to as functionally graded structures. Also, when two or more TPMS unit cell club together depending on specific functionality, it referred to as multi-morphology hybrid graded lattice structure. These structures are expected to exhibit similar morphology with host bone.

The fluid flow behavior of porous scaffold plays a crucial role in facilitating the movement of cells and guiding the formation of new tissue to promote bone ingrowth. The differentiation of these cell can be predict based on fluid velocity and shear strain. These both factors are influenced by the scaffold architecture characteristics and permeability. Permeability measures the ability of a scaffold to pass the fluids through its porous structure and support cell survival, waste removal, and nutrient transport [6]. The permeability of a scaffold mainly depends on two factors of its design: the internal geometric characteristic and porosity percentage. At same percentage of porosity, the permeability will be different for different geometric characteristic. similarly, for same type of geometry, the permeability will be different for different level of porosity percentage [7]. The scaffold also experience a shear stress due to fluid flow known as wall shear stress (WSS) [8]. WSS play a significant role in cell differentiation and proliferation. Numerous CFD analyses have been performed to evaluate the permeability and WSS. For example, Zhao et al.,[9] studied on impact of architecture characteristics on WSS. The results show that, pore size influenced the mechanical stimulation of cells within the scaffold. Santanu et al.,[10] studied on variation of cellular response with the architecture characteristic and porosity percentage. The outcomes revealed that, permeability always increases with the porosity but shows opposite trend for WSS. One most important scaffold feature is the surface area that allows for a interaction between scaffold and fluid flowing through it [11]. Thus, to understand about the scaffold performance, the fluid flow behaviour of the scaffold should be analysed. The present study comprehensively focused on two most commonly used TPMS, namely, primitive and I-graph wrapped package (IWP) minimal surface. The uniform and multi-morphology hybrid graded structures are designed to explore the influence of design characteristic on the surface area. Furthermore, a numerical simulation model was build based on COMSOL Multiphysics to understand the fluidic characteristic such as permeability and WSS of the structures.

## 2 Material and method

TPMS lattices are mathematical models of complex three-dimensional structures that have a minimal surface area when repeated in three directions. Based on the previous study, several TPMS Scaffold have been explored so far [12]. Resulting, the gyroid, primitive, IWP, and diamond were promising because of their isotropic elastic properties, high permeability, and uniform wall shear stress. Therefore, present study chosen two TPMS structures namely primitive and IWP for further studying on hybridization due to its favourability as bone implant. The structures were designed with 70% porosity at a unit cell size of 3.17 mm using an in-house developed source tool [13]. The size of each structure were kept  $12.7 \times 12.7 \times 25.4 \text{ mm}^3$  as per ASTM D695 standard size for compression test of polymer. The uniform designed structure based on primitive and IWP minimal surface are shown in Fig.1(a).

A multi-morphology hybrid graded TPMS structure can be generated by undergoing a transition between two or more minimal surfaces. For this, a weighing function 'w' was employed to assign distinct TPMS topologies to various regions within the hybrid lattice. In

mathematical terms, the following describes a simple situation involving a mixed lattice of IWP and primitive.

$$\varphi_{I+P}(x, y, z) = w[\varphi_I(x, y, z)] + (1 - w)[\varphi_P(x, y, z)] \quad (1)$$

here,  $\varphi_I(x, y, z)$  represents implicit function of first IWP lattice,  $\varphi_P(x, y, z)$  represents implicit function of second primitive lattice, and 'w' is the weighting function that determines the influence of each lattice.

The value of 'w' ranges from 0 to 1, if  $w = 0$  means only first lattice was present,  $w = 1$  means only second lattice was present, and if the values in between 0 and 1, it combined both the lattices together. 'w' can be described by a sigmoid function, for instance, such that [14];

$$w(x, y, z) = \frac{1}{1 + e^{\mu R(x,y,z)}} \quad (2)$$

In this equation,  $R(x, y, z)$  represents a set of spatial coordinates that define the geometry of the transition between distinct areas, whereas ' $\mu$ ' defines the width of that transition zone.

A new intricate design named as IWPrimwave is designed based on primitive and IWP minimal surface by setting  $R(x,y,z) = \sin x$  as shown in Fig.1(b). It is clear that IWPrimwave structure have sinusoidal transition along the x axis. This method of defining functions allows for the creation of diverse structures with distinctive characteristics.

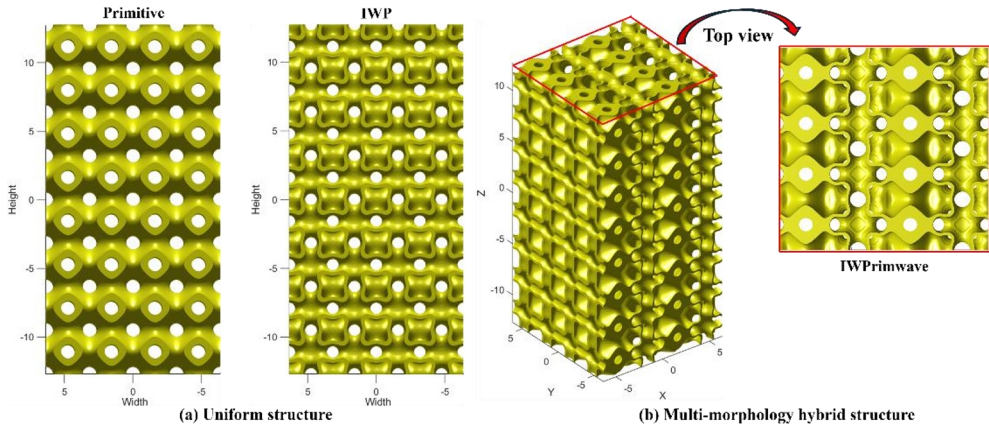


**Fig.1.** Represent (a) uniform and (b) multi-morphology structure based on TPMS minimal surface.

### 3 CFD analysis

For fluid flow simulation, a steady state computation fluid dynamic (CFD) analysis approach is considered using COMSOL Multiphysics. It helps to elucidate fluid flow pattern, permeability, and WSS distribution within the scaffold. The Navier–Stokes equation for incompressible fluid flow is used for the analysis that can be described as [15]:

$$\rho \frac{\partial u}{\partial t} - \mu \nabla^2 u + \rho(u \cdot \nabla)u + \nabla p = F, \quad \nabla \cdot u = 0 \quad (3)$$

here, p represent pressure (Pa),  $\rho$  density ( $\text{kg}/\text{m}^3$ ), u fluid velocity (m/s), F forces (N) ( $F = 0$  in present study), and  $\mu$  is dynamic viscosity ( $\text{kg}/\text{m}\cdot\text{s}$ ) respectively.

Figure 2 illustrate the CFD setup, revealing the fluid domain and the prescribed boundary conditions. Initially, a rectangular fluid domain was created, and subsequently a boolean operation was taken with respective TPMS structure as shown in Fig.2. Within the fluid domain, the surface derived from a boolean operation was set as the wall boundary, while the outer surface of the fluid domain was defined as the symmetric boundary. The Fluid flow vertically, extending from the top surface to the bottom surface of the scaffold. The pressure drops across the system was determined by establishing the outlet pressure as zero.

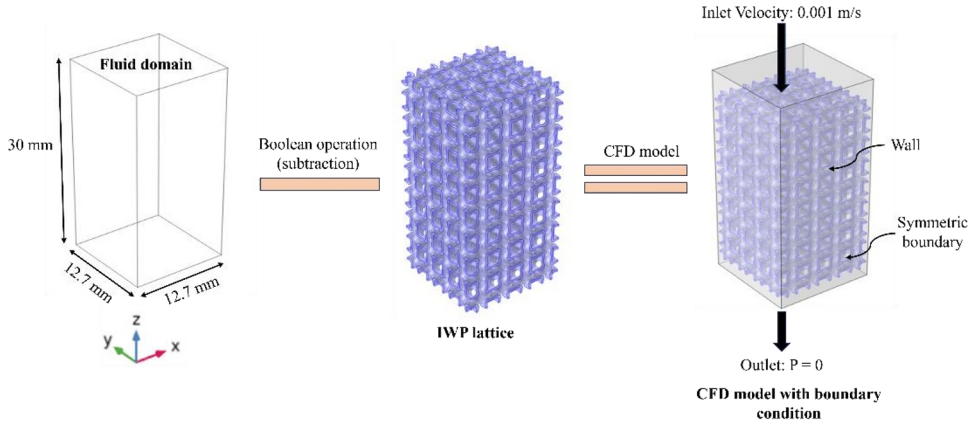


**Fig.2.** Fluid domain and boundary condition for CFD analysis.

For the analysis water is selected as the flow medium and its properties are listed in Table 1. The fluid velocity at the inlet is considered 0.001 m/s as a bone in-vivo condition [2].

Table 1. Fluid properties

Properties	Values
Density ((kg/m <sup>3</sup> ))	1000
Dynamic Viscosity (Pa.s)	0.0037

The permeability which affects the mass transportation of oxygen and nutrients, can be determined based on pressure drop using Darcy's law as [2]:

$$k = \frac{Q\mu H}{A\Delta P} \quad (4)$$

where, 'k' represents permeability (m<sup>2</sup>), 'Q' is inlet flow rate (m<sup>3</sup>/s), 'μ' is dynamic viscosity of a fluid flow (Pa.s), 'H' height of the scaffold (m), 'A' cross section area of flow (m<sup>2</sup>), and 'ΔP' is pressure drop across the scaffold structure. Another important characteristic that influences cellular behaviour is fluid-induced wall shear stress (WSS). It is a tangential stress exerted by fluid flow on the scaffold's surface. For different structures, WSS can be obtained by normal velocity gradient at wall surface as;

$$\tau_w = \mu \frac{\partial u}{\partial h} \quad (5)$$

where, 'μ' is dynamic viscosity (Pa.s), 'u' is flow velocity, and 'h' is x, y, and z direction.

## 4 Result and discussion

The permeability of the structures was affected by the architecture characteristic that differ the flow behaviour in the structures. For uniform structure, the fluid is less hindered when flowing through the scaffold, and highest permeability of  $14.3 \times 10^{-8} \text{ m}^2$  was reported in primitive structure. Meanwhile, in hybrid based IWPrimwave structure has reported permeability close to  $7.4 \times 10^{-8} \text{ m}^2$  as shown in Fig.3(a). Thus, uniform and hybrid structure, meets the requirement of natural bone ( $1.83 - 5.1 \times 10^{-8} \text{ m}^2$ ) [16]. This is not only escalating the permeability of the structures but also guarantees the transport of nutrients. Conversely, numerous pillars, transition zone, and spatially varying internal characteristic can cause lower permeability but are suitable for cell adhesion and proliferation.

To comprehend the trends in structures, the SA/V ratio of each structure was plotted, as shown in Fig.3(b). The IWP structure typically have a larger SA/V of  $7.43 \text{ mm}^2/\text{mm}^3$  among the structure. On the other hand, hybrid structure leverages the advantage of each geometric

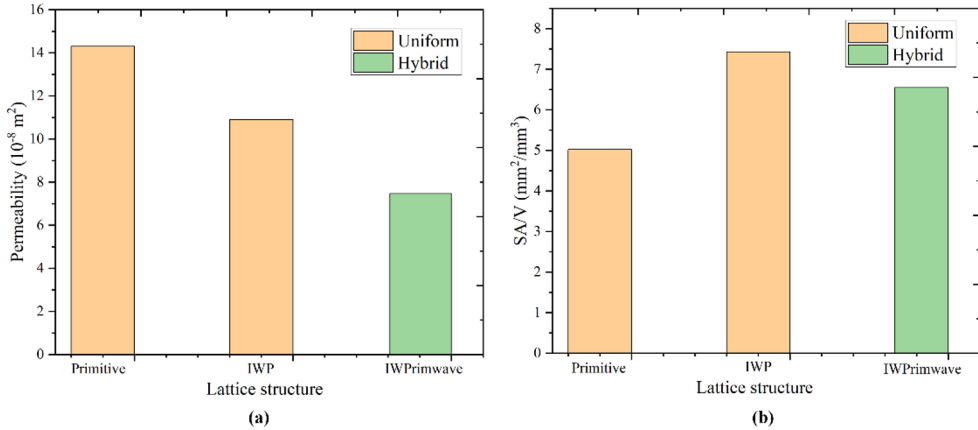


**Fig.3.** (a) permeability and (b) SA/V of uniform and hybrid graded lattice structure.

characteristic. It incorporates a lattice arrangement that maintain an intermediate SA/V ratio of 6.55 mm<sup>2</sup>/mm<sup>3</sup>, falling between the uniform structures. Thus, a hybrid graded structure effectively combine the architecture of respective TPMS minimal surface, contributing to create a tailored surface area. The value of wall shear stress varying depending upon the surface area that changes with the architecture geometry and affect the potential adhesion of bone tissue cells. The contour plot of induced fluid wall shear stress of different structures are represented in Fig.4. The wall shear stress was obtained by normal velocity gradient at the wall surface from Eq.5. As the cells adhere to the surfaces and tissue will grow over time. However, these stresses must occur at sufficient levels for bone cells, because the low and

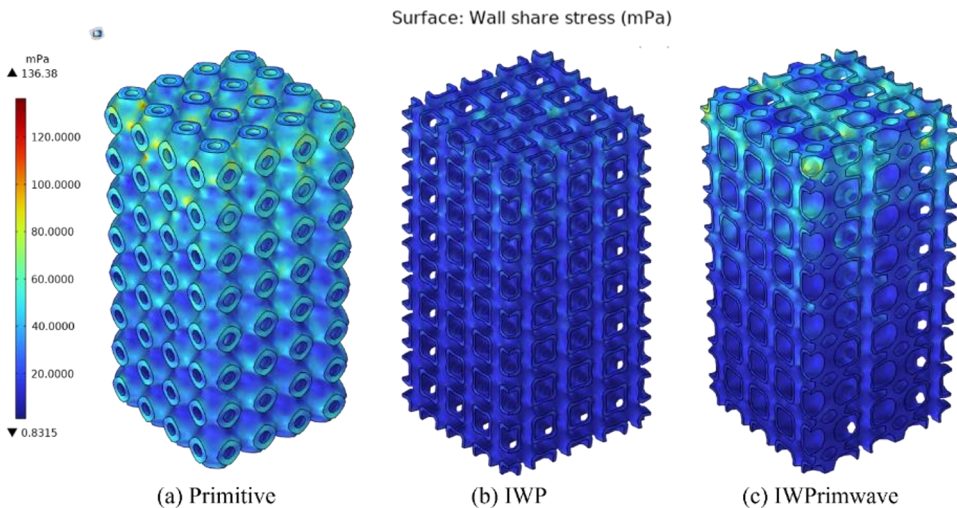


**Fig.4.** Wall shear stress contour plots of (a) primitive, (b) IWP, and (c) IWPrimwave structure.

high stresses that occur cause the death of cells or separation from the surface by occurring prevent the formation of the biomechanical environment. The average calculated WSS for uniform structure lie in a range of 0.83 – 136 mPa which is favourable to improve osteoblast differentiation and proliferation in cell seeded scaffold [17]. In multi-morphology-based hybrid graded structures, the coexistence of different architecture in a single structure, creates complex fluid patterns and wall shear stress. The average WSS induced on the surface of the

hybrid structure is lie in a range of 0.5 – 77.26 mPa, suitable to undergo chondrogenic differentiation [17].

## 5 Conclusions

The present study provides the foundation for designing scaffold based on TPMS unit cell. In the exploration of scaffold design, both uniform and hybrid structure were designed with unit cell size of 3.17 mm at 70 % porosity. For a hybrid structures design, a sigmoid function was employed to control the transition between distinct areas. The architecture characteristic of a structure plays a significant role in fluid flow behavior analysis. The new hybrid structure was comparable to natural bone with respect to complex topology but due to numerous pillars and transition zones, fluid flow was observed as a more tortuous path of streamline that affect the permeability. The estimated permeability of  $7.47 - 14.31 \times 10^{-8} \text{ m}^2$  and WSS of 0.5 – 136.88 mPa were reported in the structures are adequate for osteoblast differentiation and proliferation.

## References

1. N. Lynnerup and H.D. Klaus, “Fundamentals of human bone and dental biology”, Elsevier Inc., (2019).
2. A. Fallah, M. Altunbek, P. Bartolo, G. Cooper, A. Weightman, G. Blunn, and B. Koc, *J. Mech. Behav. Biomed. Mater.*, **134**, 105418 (2022).
3. M. Laubach, S. Suresh, B. Herath, M.L. Wille, H. Delbrück, H. Alabdulrahman, D.W. Hutmacher, and F. Hildebrand, *J. Orthop. Transl.*, **34**, 73–84 (2022).
4. H. Chen, Q. Han, C. Wang, Y. Liu, and B. Chen, **8**, 1–20 (2020).
5. O. Al-Ketan, R. Rezgui, R. Rowshan, H. Du, N.X. Fang, and R.K. Abu Al-Rub, *Adv. Eng. Mater.*, **20**, 1–15 (2018).
6. L. Polo-Corrales, M. Latorre-Esteves, and J.E. Ramirez-Vick, *J. Nanosci. Nanotechnol.*, **14**, 15–56 (2014).
7. T. Pires, J. Santos, R.B. Ruben, B.P. Gouveia, A.P.G. Castro, and P.R. Fernandes, *J. Biomech.*, **117**, 110263 (2021).
8. T. Pires, J.W.C. Dunlop, P.R. Fernandes, and A.P.G. Castro, *Proc. R. Soc. A Math. Phys. Eng. Sci.*, **478**, (2022).
9. F. Zhao, T.J. Vaughan, and L.M. Mcnamara, *Biomech. Model. Mechanobiol.*, **15**, 561–577 (2016).
10. S. Majumder, A. Gupta, S. Choudhury, and A.R. Chowdhury, **6**, 1–8 (2023).
11. O. Al-Ketan and R.K. Abu Al-Rub, *Adv. Eng. Mater.*, **21**, 1–39 (2019).
12. T. Poltue, C. Karuna, S. Khruaduangkham, S. Sechanam, and P. Promoppatum, *Int. J. Mech. Sci.*, **211**, 106762 (2021).
13. O. Al-Ketan, *Metals (Basel)*, **11**, (2021).
14. O. Al-Ketan, D.W. Lee, R. Rowshan, and R.K. Abu Al-Rub, *J. Mech. Behav. Biomed. Mater.*, **102**, 103520 (2020).
15. D. Ali and S. Sen, *J. Mech. Behav. Biomed. Mater.*, **75**, 262–270 (2017).
16. D. Yao, Z. Zhao, Y. Wei, and J. Li, *Int. J. Mech. Sci.*, **248**, 108221 (2023).
17. F. Zhao, T.J. Vaughan, and L.M. Mcnamara, *Biomech. Model. Mechanobiol.*, **14**, 231–243 (2015).